

# Determination of reflected temperature in active thermography measurements for corrosion quantification of reinforced concrete elements

Suyadi K<sup>1</sup>, Herlien D Setio<sup>2</sup>, Adang S<sup>2</sup>, Ediansjah Z<sup>2</sup>

<sup>1</sup>Civil Engineering Doctoral Program, Faculty of Civil and Environmental Engineering, ITB Bandung 40132, Indonesia

<sup>2</sup>Faculty of Civil and Environmental Engineering, ITB Bandung 40132, Indonesia

**Abstract.** This paper sums up of the determining analysis of the measuring location of  $T_{refl}$  using a thermocouple during the thermography tests. The results will be used as a reference for testing reinforced concrete corrosion by thermography method. The value and position of  $T_{refl}$  are affected by the distance between the heat source and the test objects. To study the effects of heat source magnitude variations on concrete surface temperature, the heat source is used as two halogen lamps of 500 watts each fitted at a distance of 30-50 cm. The concrete surface temperature results of quantitative image processing method are compared to the experimental test results. The results showed good accuracy, which was seen from most errors <3% and the maximum error is < 5%.

## 1. Introduction

Rebar corrosion can be detected by determining the temperature distributions on the concrete surface using an infrared camera [5]. Active thermography has been established as a method for quality monitoring [3]. Influences of rebar corrosion is to reduce its cross-sectional area and thermal coefficient of reinforced concrete around the rebar. Active infrared thermography requires an external source of energy to induce a temperature difference between defective and nondefective areas in the specimen under examination [4, 7]. When active thermography testing is carried out indoor, the effect of heat source radiation to variations room temperature will be dominant, meanwhile, room temperature fluctuations will continue to occur. As a result, there is difficulty in finding the measurement location of  $T_{refl}$  value as a correction factor.

Internal heat gain can be caused by the appliances, people, and lighting. Meanwhile, external heat gain is due to heat conduction, heat radiation, and heat gain because of ventilation [9]. Outside air temperature affects the heat transfer process in the room, through conduction mechanism in the wall. This research uses a 1000 watt halogen lamp as a heat source. The optimum irradiates were produced at a 10cm distance with a varied height between  $200\text{Wm}^{-2}$  to  $1200\text{Wm}^{-2}$  [9]. Heat transfer that occurs by radiation, conduction, and convection mechanisms. The amount of heat transfer cause of convection depends on the heat transfer coefficient ( $h_c$ ). Based on the results of research James Oliver Smith [8],  $h_c$  is dependent on wind speed ( $v$ ) as equation 1.

$$h_c = 6.22 + 8.73 v^{0.652}. \quad (1)$$

As indoor, so  $v = 0$ , then  $h_c = 6.22$  (W/m<sup>2</sup>K). Furthermore, based on the basic formula for heat transfer, radiation has the greatest effect. This will occur until the heating process is complete. This means that using halogen lamps as a heat source gives a dominant effect on the heat transfer process. The reflected temperature ( $T_{refl}$ ) used correction this noise. The amount of radiation received by an infrared camera sensor is also influenced by the transmission factor ( $\tau$ ), temperature ( $T_{atm}$ ), and the object's emissivity ( $\epsilon_{obj}$ ). The total radiation energy ( $W_{tot}$ ) received by the infrared camera sensor is a combination of object radiation and environment (atmosphere). The total radiation received by the camera like equation (2) [10].

$$W_{tot} = \epsilon_{obj} \cdot \tau \cdot \sigma (T_{obj})^4 + (1 - \epsilon_{obj}) \tau \cdot \sigma (T_{refl})^4 + (1 - \tau) \cdot \sigma (T_{atm})^4 \quad (2)$$

The transmittance of the atmosphere estimated using the distance from the object to the camera and the relative humidity [11]. The atmospheric transmission is close to 1.0 when the survey distance is small (e.g., a common distance for active IRT is from approximately 3 to 5 m). So the temperature of the object ( $T_{obj}$ ) only requires the measurement of emissivity and reflected temperature [10].  $T_{refl}$  is the same as the atmospheric temperature ( $T_{atm}$ ) for an object with high emissivity in most cases [10]. According to the handbook from FLIR Camera,  $T_{refl}$  is the same as  $T_{amb}$  [1], so  $T_{refl}$  can be written as equation (3).

$$T_{refl} = \sqrt[4]{\frac{W_{tot} - \epsilon_{obj} \cdot \sigma \cdot T_{obj}^4}{(1 - \epsilon_{obj}) \cdot \sigma}} \quad (3)$$

The thermogram is an interpretation of the heat energy received by infrared camera thermal sensors still contains noise. Some studies thermography NDT methods for corrosion of reinforced concrete as observed by Seunguk Na and Inkwan Paik (2019); David Im, et al. (2018); Hideki Oshita, et al. (2017) and Naouar L and Sougrati B (2013) use qualitative techniques for processing thermogram. In this research, represented a method for finding the position of the installation of the thermocouple around sources of heat, so the temperature is at that position as the value  $T_{refl}$  to correct the noise on the thermogram. At the end of the paper, presented experimental testing that appeared good accuracy.

## 2. Materials and methods

Emissivity ( $\epsilon_{obj}$ ) value of dry concrete is used 0.95 for this research [2]. Room temperature measurements were carried out using a data logger that was placed using the grid method per 10 cm. Halogen lamp was placed parallel to the lamp. The test carried out in the room described in figure 1. The variables used in this study are object distance ( $d_{obj}$ ), the lamp axles ( $d_{lamp}$ ), heating time ( $t_{heat}$ ), ambient temperature ( $T_{amb}$ ), and distance camera ( $d_{cam}$ ).

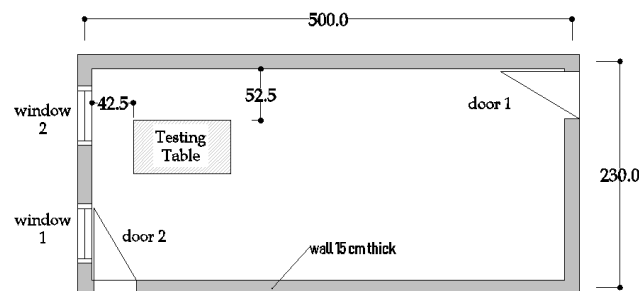
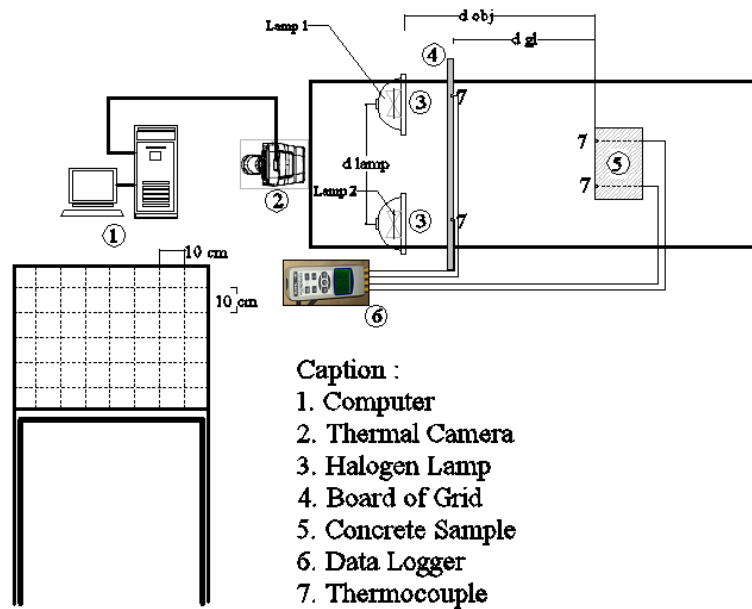


Figure 1. Laboratory room site plan

The  $T_{am}$  value in this study used 1 (one) value is  $30.6^{\circ}\text{C}$  as the initial temperature during testing ( $T_i$ ). The others variable is  $d_{cam} = (30 + d_{obj})\text{ cm}$ ;  $d_{lamp}$  is 30 cm and 35 cm. The test concrete used 20 MPa with dimensions of 10 cm x10 cm x 15 cm placed at a distance of 30 cm, 40 cm, and 50 cm in front of the heat source as showed in figure 2.



**Figure 2.** Testing the distribution of room temperature using the grid method.

Testing parameters in this research as in the table (1). Thermography testing uses a FLIR E8-XT camera with 240x360 pixels. Thermal acquisition uses the sequence recording method at a speed of 15 fps. The measurement of the concrete surface temperature during the heating phase is carried out at 2 (two) thermocouple points. Benchmarking temperature used results of thermocouple values that mounted in concrete.

**Table 1.** Test code samples by the test object distance parameter

Code	$d_{cam}$ (cm)	$d_{obj}$ (cm)	$d_{lamp}$ (cm)
T60-30	60	30	30
T70-30	70	40	30
T80-30	80	50	30
T60-35	60	30	35
T70-35	70	40	35
T80-35	80	50	35

The location of the  $T_{refl}$  determined based on the temperature distribution contour. To easy application during the experimental test, the location of the  $T_{refl}$  value measured at a distance of 10 cm in front of the halogen lamp and measured vertically from lamps 1 and 2. Tests were carried out at  $t_{heat} = 800\text{ s} - 1800\text{ s}$  with time intervals of 50 s. All the tests conducted three times.

### 3. Results and discussions

#### 3.1. $T_{refl}$ value results

Shown in figure 3, there is noise which results in concrete surface temperature difference between the results of the thermography test and the thermocouple at the same moment. This is because of the

influence of the atmosphere between the test object and the IR camera. These factors affect the value of  $\tau$  and  $T_{refl}$  in equation 2, resulting in changes in the value of  $T_{obj}$ . The  $T_{refl}$  value analysis is based on the results of the curve fitting equation of concrete surface temperature and used equation 4 with exposure time from  $t_{heat} = 800$  s — 1800 s. Used  $W_{tot} = \epsilon_{obj} \cdot \sigma \cdot T_{tot}^4$  and  $T_{tot} = T_{th}$ ;  $t = t_{heat}$ ;  $T_{obj} = T_{tc}$  so the equation (3) becomes :

$$T_{refl} = \sqrt[4]{\frac{\epsilon_{obj} \cdot \sigma \cdot T_{th}^4 - \epsilon_{obj} \cdot \sigma \cdot T_{tc}^4}{(1 - \epsilon_{obj}) \cdot \sigma}} \quad (4)$$

$T_{tc}$  and  $T_{th}$  described surface temperature data from thermocouples and thermography measurement. The value of  $T_{refl}$  is proportional to  $t_{heat}$ . Because the radiation process from halogen lamps will continue, the concrete surface will continue to absorb heat energy. Curve fitting of  $T_{refl}$  value carried out by Matlab software. The figure (3) and (4) shown the  $T_{refl}$  value increasing at T60-30 is small than at T70-30 and T80-30. The distance between the object to the light source ( $d_{obj}$ ) affects the magnitude of free space between the heat source to object.

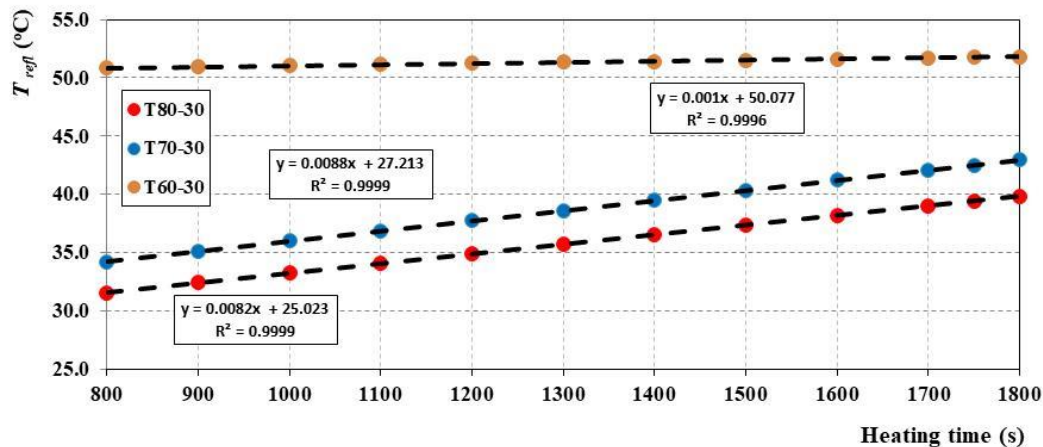


Figure 3.  $T_{refl}$  during the heating phase at several  $d_{cam}$  and  $d_{lamp} = 30$  cm

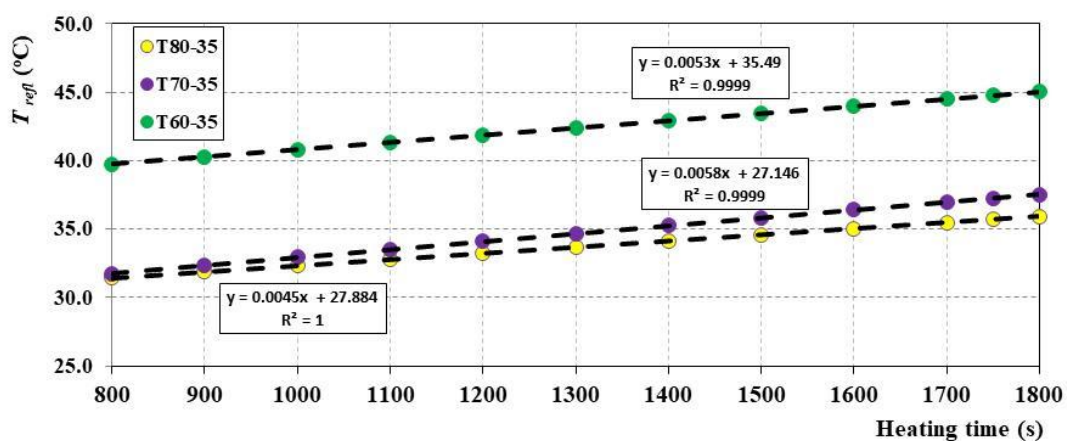


Figure 4.  $T_{refl}$  during the heating phase at several  $d_{cam}$  and  $d_{lamp} = 35$  cm

### 3.2. $T_{refl}$ location based on heating time

Results of  $T_{refl}$  location analysis used to find the thermocouple installation, where the temperature value will a noise correction parameter when quantitative analysis of the image.  $T_{refl}$  location analysis

based on a vertical distance above the lamp 1 and 2 to the temperature contour lines at  $T_{refl}$  value, which was 10 cm in front of the lamp (heat source). Analyzes were carried out for object distances of 60, 70, and 80 cm from the infrared camera. The average location result analysis of the  $T_{refl}$  test point according to heating time is shown in figure (5) and (6).

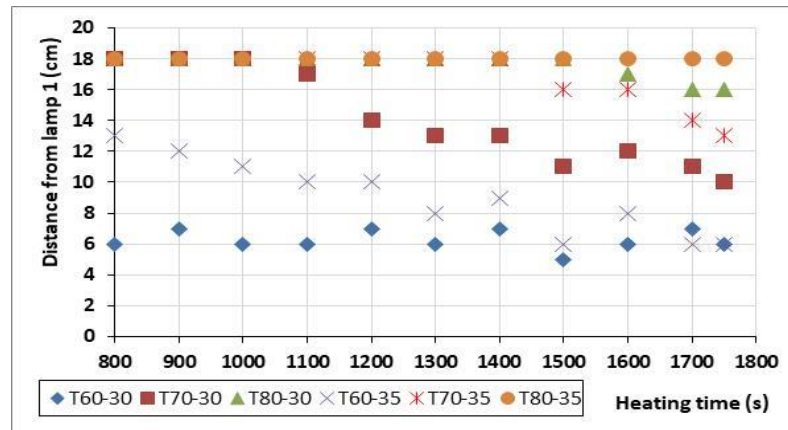


Figure 5.  $T_{refl}$  position of upper side from Lamp 1 at several  $d_{cam}$  and  $d_{lamp}$

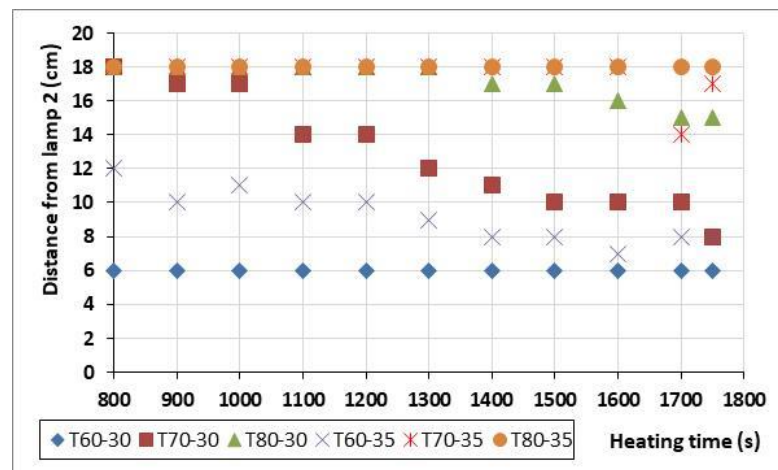


Figure 6.  $T_{refl}$  position of upper side from Lamp 2 at several  $d_{cam}$  and  $d_{lamp}$

The results of the analysis showed  $T_{refl}$  locations at T60-30 were closer than the others. It's acceptable, as lighting illuminance is inversely proportional to the square of the object's distance to the light source. Therefore, the closer the object is to the lamp, the smaller the gradient of room temperature distribution in the concrete. Increased room temperature followed by an increase in temperature of the concrete surface. This makes the  $T_{refl}$  position tend to remain constant for the irradiation time from  $t = 800 - 1800$  seconds.  $T_{refl}$  layout is 6 cm above the lamp for T60-30 meanwhile, T70-30 cm is quite various (from 7 cm until 18 cm) and T80-30 cm camera is at a distance of 18 cm. But  $T_{refl}$  layout will change if  $d_{lamp}$  is 35 cm).

#### 4. Experimental results

This test would check the reliability of the analysis result determination of  $T_{refl}$  temperature test sites to image noise correction. The  $T_{refl}$  value used to remove noise because of atmospheric conditions by equation 2, so  $T_{obj}$  as [11]:

$$T_{obj} = \sqrt[4]{\frac{W_{tot} - (1 - \epsilon_{obj}) \cdot \sigma (T_{refl})^4}{\epsilon_{obj} \cdot \sigma}} \quad (5)$$

Experimental testing was carried out by placing 2 thermocouples on the object to measure the surface temperature ( $T_{tc}$ ), and 2 thermocouples placed at the top of each halogen lamp to measure  $T_{refl}$ . Thermocouples to measure  $T_{refl}$  are installed at a distance of 10 cm in front of the lamp, with a vertical distance according to the results of the analysis of the  $T_{refl}$  location on the contour line of the room temperature distribution. Based on the regression analysis can results trendline of change equation of concrete surface temperature and room temperature ( $T_{refl}$ ) according to irradiation time ( $t$ ), when  $t = i$  and  $t$  expression as  $t_{heat}$ , so

$$T_{obj}(i) = \sqrt[4]{\frac{\epsilon_{obj} \cdot \sigma \cdot T_{th}^4(i) - (1 - \epsilon_{obj}) \cdot \sigma (T_{refl})^4}{\epsilon_{obj} \cdot \sigma}} \quad (6)$$

Based on figure (7), it can be seen that the temperature shift of the concrete surface between before and after being corrected.

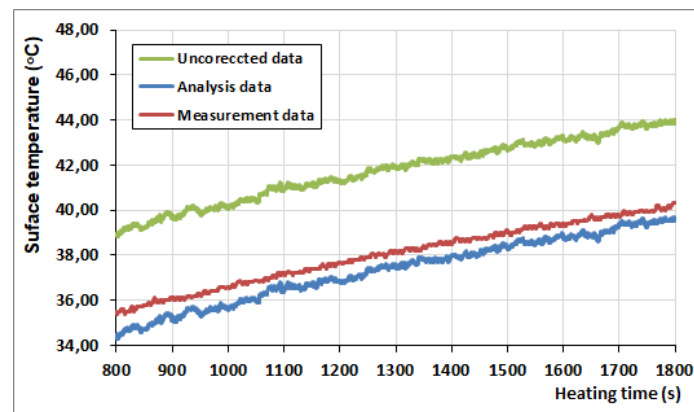
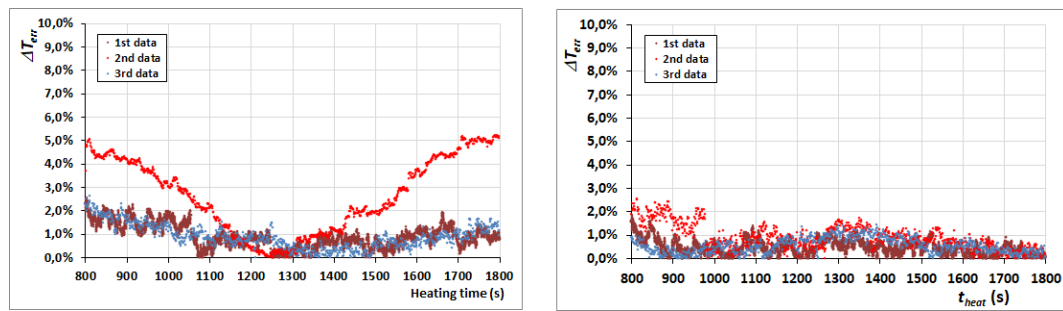


**Figure 7.** Surface temperature of concrete before and after noise correction

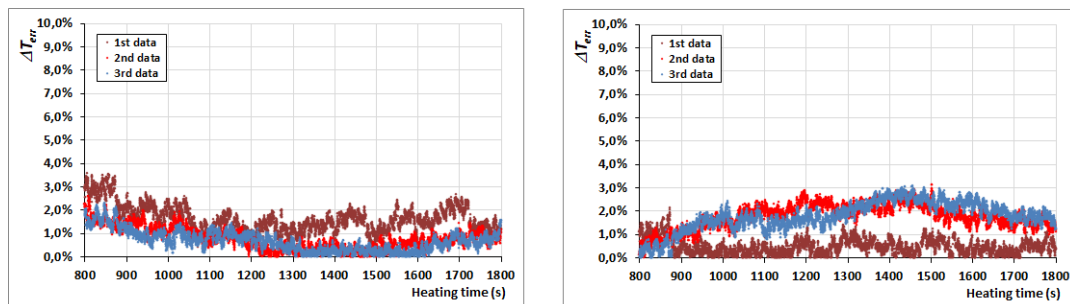
Error of analysis written as :

$$\Delta T_{err}(i) = \left[ \frac{T_{obj}(i) - T_{tc}(i)}{T_{tc}(i)} \right] \times 100\% \quad (7)$$

The results of the error analysis are depicted in below. The results show good accuracy, this can be seen from the average  $\Delta T_{err}$  error percentage is  $< 5\%$  as shown in figure (8).



a)  $\Delta T_{err}$  at point Sp1 and Sp2 on T60-30



b)  $\Delta T_{err}$  at point Sp1 and Sp2 on T70-30

**Figure 8.** The percentage of  $\Delta T_{err}$  at heating phase at several  $d_{cam}$  and  $d_{lamp}$

## 5. Conclusions

The  $T_{refl}$  value is greatest while the object is placed at a distance of 30 cm,  $d_{cam}$  is 60cm, and  $d_{lamp} = 30$ cm. The  $T_{refl}$  can be measured by thermocouples placed at 6 cm above lamp 1 and lamp 2. Meanwhile, the distance of the object is farther from the heat source, the further away the thermocouple must be installed. The closer distance of an object to the heat source, so will increase and result in smaller room temperature gradations.

## 6. References

- [1] FLIR Systems 2012 "The Ultimate Infrared Handbook for R&D Professionals"
- [2] FLIR System Inc. 2017 User's manual FLIR Ex series. Emissivity table p. 101.
- [3] Hoffmann, D., M. Bastian, and G. Schober 2020 "New approach for layer thickness measurements of coatings using pulsed lock-in thermography." Quantitative InfraRed Thermography Journal p. 1-14.
- [4] Ibarra-Castanedo, Clemente, et al. 2009 "Comparative study of active thermography techniques for the nondestructive evaluation of honeycomb structures." Research in Nondestructive Evaluation 20.1 p. 1-31.
- [5] Kobayashi, K., and N. Banthia 2011 "Corrosion detection in reinforced concrete using induction heating and infrared thermography." Journal of Civil Structural Health Monitoring 1.1-2 p. 25-35.
- [6] Moria, Hazim, T. I. Mohamad, and F. Aldawi 2016 "Radiation distribution uniformization by optimized halogen lamps arrangement for a solar simulator." J Sci Eng Res 3 p. 29-34.
- [7] Sfarra, S., et al. 2010 "A comparative investigation for the nondestructive testing of honeycomb structures by holographic interferometry and infrared thermography." Journal of Physics: Conference Series. Vol. 214. No. 1. IOP Publishing.

- [8] Smith J O 2010 Determination of the convective heat transfer coefficients from the surfaces of buildings within urban street canyons. The effect of wind speed upon convective transfer. Thesis. Department of Mechanical Engineering. University of Bath p. 186.
- [9] Suziyana, Mat Dahan, et al. 2013 "Analysis of heat gain in computer laboratory and excellent centre by using CLTD/CLF/SCL method." *Procedia Engineering* 53 p. 655-664.
- [10] Tran, Quang Huy, et al. 2017 "Effects of ambient temperature and relative humidity on subsurface defect detection in concrete structures by active thermal imaging." *Sensors* 17.8.
- [11] Usamentiaga, Rubén, et al. 2014 "Infrared thermography for temperature measurement and non-destructive testing." *Sensors* 14.7 p. 12305-12348.

### **Acknowledgments**

The authors would like to thank Bandung Institute of Technology for providing P3MI Research Grants